Fine Angle Estimation Using Weighted Average-ESPRIT for Radar-based WSN

Sangdong Kim, Yeonghwan Ju, Daegun Oh, Jonghun Lee
Daegu Gyeongbuk Institute of Science & Technology
Advanced Radar Technology (ART) Lab., Robotics System Research Division
Daegu, the republic of Korea
e-mail: kimsd728@dgist.ac.kr, yhju@dgist.ac.kr, dgoh@dgist.ac.kr, jhlee@dgist.ac.kr

Abstract—**This paper proposes a fine angle estimation using weighted average-estimation of signal parameters via rotational invariance techniques (ESPRIT) for radar-based WSN. The proposed WA-ESPRIT system is composed of a weighted average block and an ESPRIT block. The proposed system is verified through analysis, simulation and experiment. We show that the proposed system has better performance than the conventional one. The performance of the proposed algorithm is verified through Monte-Carlo simulations in an additive white Gaussian noise (AWGN).**

Keyword-radar-based WSN; Monitoring system; Weighted-average scheme; ESPRIT.

I. INTRODUCTION

Historically, surveillance systems have used infrared, acoustics and magnetics for passive sensing, and optics and ultrasounds for active sensing, but radio detection and ranging (radar) has been conspicuously absent. Conventional radar systems such as the pulse Doppler radar and the frequency modulated continuous-wave (FMCW) radar employ transmitted and reflected microwaves to detect, locate, and track objects over long distances and large areas. Due to its ability, radar has found applications in defense and remote sensing. However, widespread commercial applications of the radar have been limited because conventional systems are expensive, bulky and difficult to use. The radar motion sensors which have a short range and poor false alarm rates is used in unstructured environments such as traffic monitoring and police radar [1]. Since many wireless sensor networks (WSN) operate in unstructured environments with limited energy supplies, these conventional sensors are unsuitable for WSN. The FMCW radar is mostly used to gather traffic data information such as lane position and for radar-based WSN because the radar detects the angle between the target and the radar. The advantage of the FMCW radar is to obtain simple hardware architecture, lower peak level and low-cost comparing with pulse radar [2].

Among various estimated parameter such as distance and angle in radar detectors, the angle estimation is focused because the angle error is directly depended on the lane detection of the vehicle. Conventional angle estimation method show that parametric methods such as MUSIC, estimation of signal parameters via rotational invariance techniques (ESPRIT) and matrix pencil (MP) are used for super-resolution frequency estimation algorithms [3-5]. However, since conventional super-resolution method has assumed a lot of antenna arrays, the conventional one cannot operate well in case of a few arrays such as 2 or 3 arrays. Therefore, we propose weighted average (WA)-ESPRIT for low complexity realization of high resolution radar-based WSN. This paper is organized as follows. In Section 2, we introduce the system model for FMCW radar. Section 3 proposes WA-ESPRIT for the angle estimation, while Section 4 discusses the performance analysis of the WA-ESPRIT radar based on various parameters. Section 5 shows the simulation results for WA-ESPRIT radar and Section 6 shows experiments to testify the effectiveness of the proposed estimation. Finally, Section 7 concludes our proposed estimation with high resolution under real channel.

II. SYSTEM MODEL

The signal model of FMCW radar is expressed in this section. The transmitted FMCW chirp signal can be represented by

$$s(t)=\begin{cases}\exp\left[j\left((\omega_s+\omega_c)t+\frac{\mu}{2}t^2\right)\right] & \text{for } 0\le t<T_{sym} \\ 0 & \text{elsewhere}\end{cases}. \quad \textbf{(1)}$$

where ω_s denotes the start frequency, ω_c denotes the carrier frequency, μ is the rate of change of the instantaneous frequency of a chirp signal, and T_{sym} is the duration of chirp signals. The relation between the bandwidth of FMCW transmitted signal and μ is expressed by $\omega_{BW}=\mu T_{sym}$.

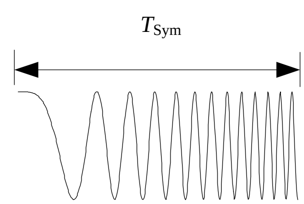

(a) Transmitted signal

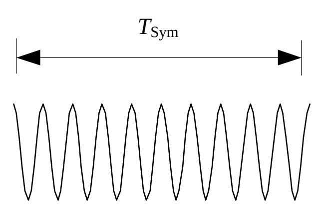

(b) Dechirping signal of received signal

Figure 1. The signal scheme of FMCW radar signal

Consider M targets receiving at K antenna arrays. Let ϕ_m and τ_m denote the angle and delay of target of the m-

th target. The received signal at each antenna array can be represented by

$$r_k(t) = \sum_{m=0}^{M-1} a_m \exp\left(j\frac{2\pi}{\lambda} d\left(k-1\right)\sin\phi_m \right) s\left(t-\tau_m\right) + w_k(t) \quad (2)$$

where a_m denotes the complex amplitude for the m-th target, λ denotes the wave-length of the carrier signal, d is the spacing between the adjacent antenna elements, and $w_k(t)$ is the additive white Gaussian noise (AWGN) signal at the k-th antenna element.

In FMCW radar, received chirp signals can be easily transformed into the sinusoidal waveform by de-chirping as shown in Figure 1. Omitting AWGN signal, the sinusoidal signals of the received signal can be represented by

$$y_k\left(t\right) = \sum_{m=0}^{M-1} a_m \exp\left(j\frac{2\pi}{\lambda} dk\sin\phi_m \right) \exp\left(j\left(\mu\tau_m t - \frac{\mu}{2}\tau_m{}^2 + \omega_c\tau_m \right)\right). \quad (3)$$

After analog-to-digital conversion (ADC), the discrete time model of (3) satisfying Nyquist sampling can be derived by $y_k[n]=y_k(nT_s)$ for n=0,...,N-1.

III. WEIGHTED AVERAGE - ESPRIT

In this section, we show that the WA-ESPRIT is employed for the fine distance estimation of the received signal and that the proposed estimator combines the ESPRIT with a weighted average scheme by considering the signal-to-noise ratio (SNR) of the received signal.

A. ESPRIT

The ESPRIT can be represented as follows. Let $\mathbf{Y}=[y_1[n],..., y_K[n]]^T$ can be a set of snapshots from K antenna arrays. Then, autocorrelation matrix $\boldsymbol{R_k}$ can be expressed by

$$\boldsymbol{R} = \sum_{n=0}^{N-1} \boldsymbol{YY}^H \quad (4)$$

The eigenvalue decomposition (EVD) of the autocorrelation matrix $\boldsymbol{R}$ has the form given by

$$\boldsymbol{R} = \left[\boldsymbol{S}_{N\times M} \quad \boldsymbol{G}_{N\times(N-M)} \right] \begin{bmatrix} \lambda_0 & & \\ & \ddots & \\ & & \lambda_{L-1} \end{bmatrix} \begin{bmatrix} \boldsymbol{S}^*{}_{N\times M} \\ \boldsymbol{G}^*{}_{N\times(N-M)} \end{bmatrix} \quad (5)$$

where signal eigenvector matrix $\boldsymbol{S}=[s_0, \ldots, s_{M-1}]$ contains M eigenvectors which span the signal subspace of the correlation matrix, noise eigenvector matrix $\boldsymbol{G}=[g_0, \ldots, g_{N-M-1}]$ means N-M eigenvectors spanning the noise subspace of the correlation matrix and λ_n denotes a n-th eigenvalues of the correlation matrix. The largest M eigenvalue $\lambda_{0,\ldots,}\lambda_{M-1}$ correspond to the M eigenvectors of $\boldsymbol{S}$. The other eigenvalue λ_M ... λ_{L-1} correspond to the eigenvectors of $\boldsymbol{G}$ such that $\lambda_M = \ldots = \lambda_{L-1}=\sigma^2$. Let us define $\boldsymbol{S}_1$ and $\boldsymbol{S}_2$ matrix, which is $\boldsymbol{S}_1=[\boldsymbol{I}_{m-1}\ \mathbf{0}]\boldsymbol{S}$ and $\boldsymbol{S}_2=[\mathbf{0}\ \boldsymbol{I}_{m-1}]\boldsymbol{S}$. The sub-matrices, which showed in [11] , are factorized by

$$\boldsymbol{S}_1 = \boldsymbol{A}_1\boldsymbol{C} \text{ and } \boldsymbol{S}_2 = \boldsymbol{A}_1\boldsymbol{DC} = \boldsymbol{S}_1\phi \quad (6)$$

where $\boldsymbol{A}_1=[\boldsymbol{I}_{m-1}\ \mathbf{0}]\boldsymbol{A}$, $\boldsymbol{D}$=diag[$\delta_{0,\ldots,}\delta_{M-1}$], δ_m denotes the frequency of the transformed sinusoid for the m-th path (i.e. $\delta_m=\mu\tau_m T_s$), $\phi = \mathbf{C}^{-1}\mathbf{DC}$ and $\boldsymbol{C}$ denotes the non-singular transformation matrix of M by M. So ϕ has the same eigenvalues as $\boldsymbol{D}$. ϕ is uniquely determined given by

$$\phi = (\boldsymbol{S_1}^*\boldsymbol{S_1})^{-1}\boldsymbol{S_1}^*\boldsymbol{S_2} \ . \quad (7)$$

Among the number of ϕ, the first angle estimate is found by

$$\hat{\phi} = \sin^{-1}\left(\frac{1}{\pi}\angle(v_1)\right) \quad (8)$$

where $\angle(\cdot)$ means the phase angles for a complex signal and v_1 are first eigenvalue of ϕ.

B. Weighted Average Scheme

From (3), when the channel is not varied in processing time, the WA-ESPRIT exactly estimated the angle frequency that is affected by noise. When the power of the received signal is applied to weighted average scheme, the proposed WA-ESPRIT has better performance.

To estimate a frequency that is affected by noise, a weighted average angle frequency is expressed using

$$\hat{\phi}_{WA} = \sum_{i=0}^{L-1} \hat{\eta}_i \hat{\phi}_i \quad (9)$$

where η_i denotes the signal power of i-th received signal, $\hat{\phi}_{wa}$ is the proposed angle estimation result.

IV. PERFORMANCE ANALYSIS OF THE WA-ESPRIT RADAR

This section analyzes the performance of the WA-ESPRIT radar. When the receiver is assumed to be perfectly received without unwanted frequency, the detection probability of the coherent receiver can be given by Equation (10) and (11) [5].

$$P_D = Q(Q(P_{FA}) - \sqrt{N \cdot SNR}) \quad (10)$$

$$Q = \int_x^\infty \frac{1}{\sqrt{2\pi}} \exp\left(-\frac{1}{2}t^2\right)dt \quad (11)$$

where P_{FA} and P_D denote the false alarm rate and detection probability, respectively. In order to evaluate the detection probability of the proposed radar receiver, we assume that the FFT and the square block of received signal have same distribution characteristics as those of the square of the Gaussian random variable. If received signal represents noise alone, then the probability density functions of noise can be calculated at the receiver as

$$p_0\left(y_k\right)=\frac{1}{\sigma^n 2^{n/2}\Gamma\left(\frac{1}{2}n\right)}\,{y_k}^{(n/2)-1}e^{-D/2\sigma^2} \quad (12)$$

where the n degree central chi-square distribution with zero mean and variance σ^2 and $\Gamma\left(n\right)$ is the gamma function. Then, when a received signal is existed with signal and noise, then the probability density functions of y_k can be calculated at the receiver output as

$$p_1\left(y_k\right)=\frac{1}{2\sigma^2}\left(\frac{y_k}{s^2}\right)^{(n-2)/4}e^{-(s^2+y_k)/2\sigma^2}I_{(n/2)-1}\left(\sqrt{y_k}\,\frac{s}{\sigma^2}\right) \quad (13)$$

where the n degree non-central chi-square distribution with s^2 mean and variance σ^2 and $I_\alpha\left(x\right)$ is the α th-order modified Bessel function of the first kind. The probability of false alarm, P_{fa}, is defined as the probability that a sample $y_k[n]$ will exceed the defined threshold when noise alone is present in the radar receiver,

$$P_{fa}=\int_T^\infty \frac{1}{\sigma^n 2^{n/2}\Gamma\left(\frac{1}{2}n\right)}\,{y_k}^{(n/2)-1}e^{-y_k/2\sigma^2}dy_k \quad (14)$$

where the n degree is the same as the N-point FFT and T is the defined threshold level. The probability of detection, P_D, is the probability that a sample $y_k[n]$will exceed the defined threshold in the case of noise plus signal in the radar receiver,

$$P_D=\int_T^\infty \frac{1}{2\sigma^2}\left(\frac{y_k}{s^2}\right)^{(n-2)/4}e^{-(s^2+y_k)/2\sigma^2}I_{(n/2)-1}\left(\sqrt{y_k}\,\frac{s}{\sigma^2}\right). \quad (15)$$

The relation between the detection probability and the false alarm rate of the squared non-coherent receiver is analyzed with N-point FFT, as in Eq. (12) such that

$$\begin{aligned}P_D &= Q(Q^{-1}(P_{FA}/2)-\sqrt{N\cdot SNR})\\ &+Q(Q^{-1}(P_{FA}/2)+\sqrt{N\cdot SNR})\end{aligned}\quad . \quad (16)$$

V. SIMULATION RESULTS

We present Monte-Carlo simulation results averaged over 10,000 estimates to evaluate the performance of the proposed algorithm. The angle estimation performance of the proposed algorithm is compared with that of the conventional algorithms such as ESPRIT-based angle estimation algorithm. This paper only takes into account the RMSE for single tone frequency. In the following simulations, we normally adopt the FMCW radar system with M=3 and K=4.

In Figure 2, the proposed algorithm is compared to other algorithms such as DFT and ESPRIT. Here, δ means the fractional number of the angle frequency. In case of M =3, the RMSE of the proposed algorithm has better performance than that of the ESPRIT at every angle frequency.

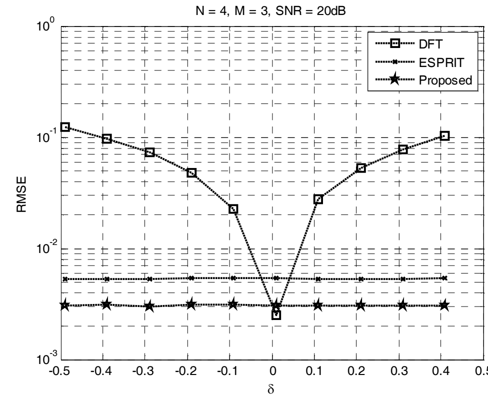

Figure 2. Performance comparison of the proposed method in various angle

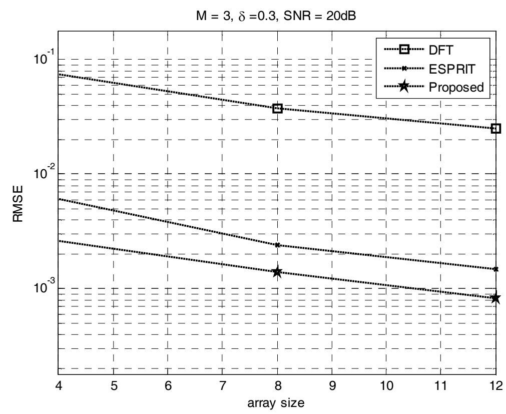

Figure 3. Performance comparison of the proposed algorithm for various antenna arrays K

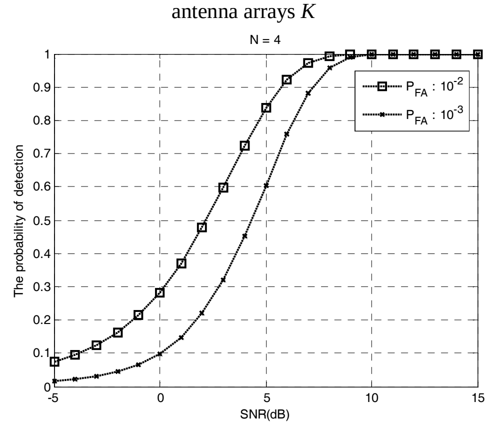

Figure 4. Performance comparison of the proposed algorithm for various false alarm rate

Figure 3 shows the RMSE of various estimators according to increasing of the sample N. For the change of the array size K, K increases from 4 to 12. When K increases, the RMSE of the proposed estimator improves. In particular, in the case of the proposed estimator, when N changes from 4 to 12, the RMSE characteristics improve by more than about 3 times, with a change from 2.59e-3 to 0.82e-3. Figure 4 shows the performance comparison of the proposed algorithm for various false alarm rates. After

 ISBN: 978-1-61208-398-8

SNR=10dB, the detection probability of P_{FA} =10^{-2} and 10^{-3} is same.

VI. EXPERIMENTS

In order to testify the effectiveness of the proposed estimation in a real environment, at Daegu-Gyeongbuk Institute of Science & Technology (DGIST) in Korea, we fulfilled various experiments in an anechoic chamber. We implemented a 24 GHz FMCW RF module which included a transmitting/receiving channel. The transmitter contained a voltage controlled oscillator (VCO), a frequency synthesizer, and a 26MHz oscillator used as the input of VCO. A frequency synthesizer controlled the input voltage of the VCO in order to generate the FMCW source. The source swept over the range of 24.05-24.25 GHz, i.e., a 200 MHz bandwidth. The receiver consisted of three LNAs, three mixers, three high-pass filters (HPFs) and three low-pass filters (LPFs). The receiver had an overall noise figure of 8 dB. The gain and noise figure of the LNAs were 14 dB and 2.5 dB, respectively. An RF signal was down-converted to an IF signal (beat signal) by the mixer.

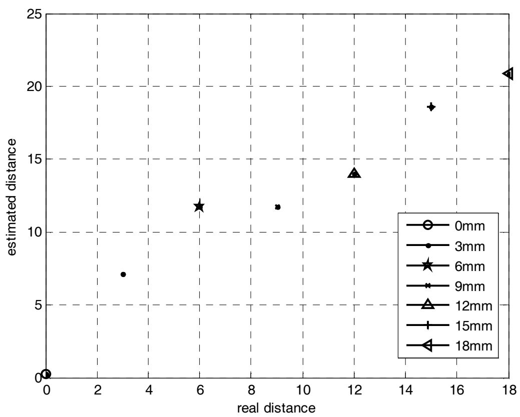

Figure 5. Experimental results

We verified the performance of the proposed method for various distance between radar and target in the chamber. When a target were placed at R=[0, 3, 6, 9, 12, 15, 18]mm for precise estimation in the anechoic chamber, respectively, the range map was derived as in Figure 5, where each colored dot indicates an estimation result. The proposed method can estimate the TOAs of various distances well.

VII. CONCLUSION

This paper proposed the fine angle frequency estimation system for radar-based WSN that takes into consideration the WA-ESPRIT. In order to improve the accuracy of the angle frequency estimation, the proposed algorithm applied a weighted average scheme according to the average signal amplitude of the received signal. We illustrate that the proposed estimator has better performance than the ESPRIT at M=3 and improves by more than about 3 times from K=4 to 2. In the future, we will make the various outdoor experiments.

ACKNOWLEDGMENT

This work was supported by the DGIST R&D Program of the Ministry of Science, ICT and Future Planning, Korea (15-RS-01) and the Ministry of Trade, Industry & Energy(MOTIE), Korea Institute for Advancement of Technology(KIAT) and DaeGyeong Institute for Regional Program Evaluation(DGIRPE) through the Leading Industry Development for Economic Region.

REFERENCES

[1] P. K. Dutta, A. K. Arora and S. B. Bibyk, “Towards radar-enabled sensor networks,” in Proc. 5th Int. Conf. Information Processing SensorNetworks (IPSN), Nashville, TN, Apr. 2006, pp. 467–474.

[2] M. S. Lee and Y. H. Kim, "Design and Performance of a 24-GHz Switch-Antenna Array FMCW Radar System for Automotive Applications," IEEE Transactions on Vehicular Technology, vol.59, no.5, pp.2290-2297, Jun 2010

[3] A. N. Lemma, A. J. Vanderveen and E.F. Deprettere, “Multiresolution ESPRIT Algorithm,” IEEE Transactions on Signal Processing, vol. 47, pp. 1722-1726, Jun. 1999.

[4] T. K. Sarkar and O. Pereira, “Using the matrix pencil method to estimate the parameters of a sum of complex exponentials,” IEEE Antennas Propagator Magazine, vol.37, pp.48–55, Feb. 1995.

[5] X. Li and K. Pahlavan, “Super-Resolution TOA Estimation With Diversity for Indoor Geolocation,” IEEE Trans. on Wireless Comm., vol. 3, pp. 224–234, Jan. 2004.

ISBN: 978-1-61208-398-8